Polym. Korea, Vol. 50, No. 3, pp. 451-460 (2026)
https://doi.org/10.7317/pk.2026.50.3.451
ISSN 2234-8077(Online)

BTPPC 삽입형 운모를 활용한 PCTG의 열적, 기계적 특성 및 치수 안정성 향상

Xiang Li†, Guirong Xie, Jiaxin Cheng, and Sheng Zhong
Hunan Chemical Vocational Technology College
(2025년 11월 19일 접수, 2026년 4월 8일 수정, 2026년 4월 8일 채택)

Improving Thermal, Mechanical, and Dimensional Stability of PCTG Using BTPPC-Intercalated Muscovite

Xiang Li†, Guirong Xie, Jiaxin Cheng, and Sheng Zhong
Hunan Chemical Vocational Technology College, Zhuzhou 412000, China
(Received November 19, 2025; Revised April 8, 2026; Accepted April 8, 2026)

Abstract: In order to enhance the properties of poly(1,4-cyclohexylene dimethylene terephthalate) (PCTG), organic muscovite (O-Mus) which was prepared by intercalating benzyl triphenyl phosphorus chloride (BTPPC) into muscovite (Mus) was used as a functional filler for PCTG , and a series of PCTG/O-Mus composites were prepared. The properties of the PCTG composites were analyzed by FTIR, XRD, SEM and DMA. The results showed that BTPPC could successfully intercalated into Mus layers. When the addition amount of O-Mus was 2%, 4%, and 6%, the O-Mus was mainly in a delaminated state and well dispersed in PCTG.The dimensional stability, hot deformation temperature (HDT), vicat softening temperature (VST), thermal decomposition temperature and flexural modulus of PCTG/O-Mus increased with increasing the content of O-Mus. The post-moulding shrinkage of PMD and NMD of PCTG/O-Mus-6 were 0.63% and 0.49%, respectively, which were 38.2% and 42.4% lower than those of PCTG. The HDT, VST, initial decomposition temperature ($T_{5\%}$) and the temperature at the maximum mass loss rate (T_{max}) of PCTG/O-Mus-6 were 94 °C, 103 °C, 423.8 °C, and 460.1 °C, respectively, which were 12 °C, 12 °C, 22.6 °C, and 37.8 °C greater than those of PCTG. The flexural and tensile strengths of PCTG/O-Mus increased at first, and then decreased. Adding O-Mus could increase the glass transition temperature of PCTG, and with the increase of O-Mus addition, the glass transition temperature of PCTG/O-Mus is higher.

Keywords: poly(1,4-cyclohexylene dimethylene terephthalate), organic muscovite, benzyl triphenyl phosphorus chloride, post-moulding shrinkage, mechanical properties.

Introduction

Poly(1,4-cyclohexylene dimethylene terephthalate) (PCTG) is a thermoplastic polyester formed by the polycondensation of terephthalic acid and cyclohexanedimethanol.[1] PCTG exhibits excellent viscosity, transparency, colorability, processability, and chemical resistance, making it suitable for manufacturing industrial products with high precision requirements and complex structures.[2] Its products exhibit high transparency and excellent impact resistance, making them particularly suitable for manufacturing thick-walled transparent products. Unlike polycarbonate (PC), PCTG is bisphenol A-free and poses no health risks.[3] However, the dimensional stability, heat deflection temperature (HDT), and flexural modulus of PCTG are poor, which limits its application. Therefore, finding ways to improve the dimensional stability, heat deflection temperature, and flexural modulus of PCTG is significant.

Layered inorganic silicate materials can effectively enhance the mechanical properties, thermal performance, and dimensional stability of polymers when well dispersed, owing to their high rigidity, excellent heat resistance, and high aspect ratio.[4-12] Moreover, compared with conventional inorganic reinforcing materials, they can significantly improve polymer properties even at low loading levels.[13-16] In recent years, these materials have attracted extensive research attention in both academic studies and industrial applications.[17-22] Muscovite (Mus), as well

†To whom correspondence should be addressed.
iverson25@126.com, ORCID 0000-0002-1394-3759
©2026 The Polymer Society of Korea. All rights reserved.

as VMT, is a mica-type silicate and possesses a layered structure. Each layer consists of octahedrally coordinated cations (typically Mg, Al, and Fe) sandwiched by tetrahedrally coordinated cations (typically Si and Al).[23,24] Owing to its chemical and mechanical stability, the layered Mus has been widely used in a variety of applications, including wear-resistant agent,[25] conductive conductor agent[26] and reinforcing filler of polymers.[27,28] Generally, to achieve significant improvements in mechanical and thermal properties of polymers through inorganic particle incorporation, good dispersion of the particles within the polymer matrix must first be ensured. Therefore, organic modification of inorganic particles is commonly employed to enhance their organic affinity, thereby improving interfacial adhesion between the particles and polymer matrix.[29,30] If muscovite can be organically modified and exfoliated into flakes with larger specific surface area and improved compatibility, it may yield unexpected effects in enhancing polymer performance. However, little literature exists so far on this topic.

This study aims to investigate the effect of benzyl triphenyl phosphorus chloride (BTPPC) modified muscovite on the properties of PCTG. It is anticipated that BTPPC-modified Mus may enhance the mechanical properties, thermal properties, and dimensional stability of PCTG, as it can achieve an exfoliated state and disperse uniformly within the PCTG matrix. Analyses were conducted on PCTG control samples, PCTG/Mus composites, and PCTG/O-Mus composites. Sample characterization employed microscopic and spectroscopic techniques, including fourier transform infrared spectrometer (FTIR), x-ray diffraction (XRD), and scanning electron microscope (SEM). Composite properties were evaluated using a universal testing machine, dynamic thermo-mechanical analyzer, and thermal deformation vicat softening point tester. The original contribution of this work lies in the innovative utilization of BTPPC modified Mus to enhance PCTG performance—a solution first proposed in the field of materials science. Results indicate that BTPPC was successfully intercalated into the Mus interlayers, d the interlayer distance of Mus achieved an exfoliated state of Mus in PCTG, enhancing the performance of PCTG. This finding holds significant implications for fabricating high-performance PCTG, broadening its application scope, and provides new research directions for future organic modification of Mus.

Experimental

Materials. PCTG was purchased from Eastman USA LTD (Tennessee, USA); Benzyl triphenyl phosphorus chloride (BTPPC, the effective substance content was, ≧99%) was purchased from Shanghai Ruichu Biotechnology Co., LTD (Shanghai, China). Muscovite (Mus, < 1 um) was purchased from Hebei Lingshou Micro-mineral Co., Ltc; Antioxidant 168 was purchased from BASF, Germany; Antioxidant 1010 was purchased from Basf Of Germany.

Preparation of Organic Muscovite (O-Mus). The muscovite was first calcined in a 700° muffle furnace for 2 hours, then naturally cooled and dispersed in distilled water, and then BTPPC was slowly added under the condition of constant agitation. After the BTPPC was completely dissolved, the mixture was ultrasonicated for 5 hours and refluxed in the water bath at 80 °C for 12 hours, and then filtered, washed, dried, and sifted by 12500 mesh sieve to obtain the organized muscovite (O-Mus).

Preparations of Samples. The formulations and abbreviations of various composites are listed in Table 1. PCTG, Mus, O-Mus, 168, and 1010 were first premixed in a high-speed mixer. The composites were then melt-extruded using a twin-screw extruder at barrel temperatures of 220/230/235/240/245/245/245 °C with a screw speed of 350 rpm to prepare composite pellets. Subsequently, the pellets were injection-molded into ISO standard specimens at 220-250 °C.

Fourier Transform Infrared Spectrometer (FTIR). Fourier transform infrared spectrometer (FTIR) spectra between 400 and 4000 cm^{-1} were obtained on a spectrometer (Nicolet 6700, Beijing Keai Bao Technology Development Co., LTD, China).

X-ray Diffraction (XRD). X-ray diffraction (XRD) patterns were recorded on a diffractometer (MSAL-XD2, Bragg Tech-

Table 1. Formulations and Abbreviations of Various Composites

Samples	PCTG (%)	Mus (%)	O-Mus (%)	1010 (%)	168 (%)
PCTG	99.1	0	0	0.6	0.3
PCTG/Mus-4	95.1	4	0	0.6	0.3
PCTG/O-Mus-2	97.1	0	2	0.6	0.3
PCTG/O-Mus-4	95.1	0	4	0.6	0.3
PCTG/O-Mus-6	93.1	0	6	0.6	0.3
PCTG/O-Mus-8	91.1	0	8	0.6	0.3

nology (Beijing) Co., LTD, China) using graphite monochromatic Cu Kα radiation (λ = 0.1541 nm) at a generator voltage of 40 kV and a current of 40 mA; measurements were conducted within a 2θ range of 2.0-50.0° at a scanning rate of 1°/min.

Scanning Electronic Microscope (SEM). The fractured specimens were sputter-coated with gold three times (20 s each), and after drying, SEM images were obtained using a scanning electron microscope (XL-30, Philips, Netherlands) at an accelerating voltage of 20.0 kV.

Dynamic Thermo-mechanical Properties Test (DMA). The dynamic thermo-mechanical properties were measured using a dynamic mechanical analyzer (DMA242, Nach SCIENTIFIC Instrument TRADING (Shanghai) Co., LTD, China) equipped with a three-point bending fixture (span length: 40 mm). The measurements were conducted from room temperature to 150 °C at a heating rate of 5 °C/min, with a frequency of 1 Hz and amplitude of 25 μm.

Dimensional Stability. The dimensional stability of the materials are expressed by the post-moulding shrinkage. The post-moulding shrinkage test was conducted as per ISO standards 294-4: 2019. The tests were made in quintuplicate and the results were reported as average.

Hot Deformation Temperature (HDT) and Vicat Softening Temperature (VST). The hot deformation temperature of the materials was expressed by temperature of deflection under load. The temperature of deflection under load test was conducted as per ISO standards 75-1: 2013. The tests were made in quintuplicate and the results were reported as average.

Thermogravimetry Analysis. Thermogravimetric analysis (TG) of the samples under nitrogen atmospheres was performed on a TAQ50 apparatus (TA Instruments Inc., USA). All the samples were heated from room temperature to 750 °C at the rate of 10 °C/min.

Mechanical Properties. The tensile properties of the composites were tested using a Universal Testing Machine (LLOYD LR100K) according to ISO 527-1, with type 1A specimens at a tensile speed of 5 mm/min. The flexural properties were measured using a Universal Testing Machine (LLOYD LR100K) following ISO 178, employing specimens with dimensions of 80 mm × 10 mm × 4.0 mm at a loading rate of 2 mm/min. The notched impact strength was determined using an impact testing machine (ZBC-50) according to ISO 8256, with a pendulum energy of 5.5J, type A notch, and impact velocity of 3.5 m/s.

Light Transmittance. The light transmittance of the composites were tested using a Single-beam photometer (722N, Shandong Derike Instrument Co., Ltd, China) according to ISO 13468-1, employing specimens with dimensions of 50 mm × 50 mm × 1.0 mm.

Chemical Resistance. The chemical resistance of the composites according to ISO 175, employing specimens with dimensions of 60 mm × 60 mm × 1.0 mm. Test conditions: pH = 11, 5 days.

Results and Discussion

FTIR Spectra. From the Figure 1, it could be seen that the main infrared absorption peaks of Mus was 3630 cm^{-1}, 3436 cm^{-1}, 1645 cm^{-1}, 1430 cm^{-1}, 1022 cm^{-1} and O-Mus had additional absorption peaks at 2940 cm^{-1}, 2822 cm^{-1}, 1480 cm^{-1}, and 783 cm^{-1} compared with Mus, the functional group corresponding to infrared absorption frequency of Mus and O-Mus were illustrated in Table 2. The result indicated that the benzyl triphenyl phosphorus chloride has entered Mus. In order to confirm the benzyl triphenyl phosphorus chloride were intercalated into the layers of Mus, XRD analysis was carried out.

XRD Analysis. The characteristic peaks of X-Ray Diffraction would shift if the layer spacing of layered fillers was changed according to Bragg's Law equation (2d sinθ=nλ), and the smaller the θ, the bigger the spacing between the layers. Figure 2 illustrated the X-Ray Diffraction of Mus and O-Mus. It can be seen that the 2θ value of O-Mus (a) is lower than that of Mus (b), which indicates that the layer spacing of Mus has increased and that benzyl triphenylphosphorus chloride has been successfully intercalated into the interlayer of Mus.

It can be seen from Figure 3 that there were characterstic peaks of Mus in PCTG/Mus-4 (b), meaning that Mus retained

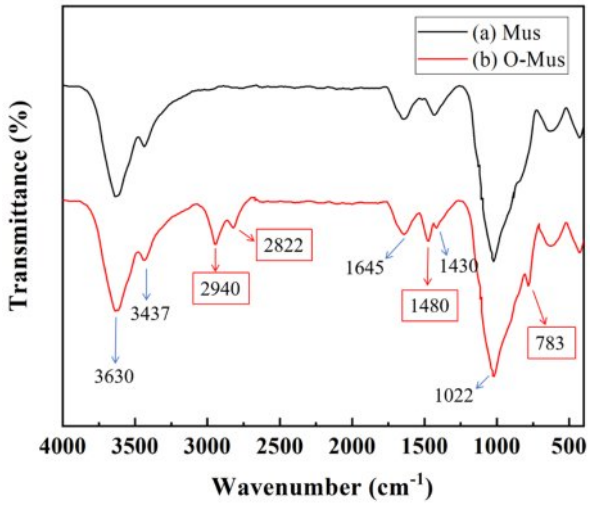

Figure 1. FTIR spectra of (a) Mus; (b) O-Mus.

Table 2. The Functional Group Corresponding to Infrared Absorption Frequency of Mus and O-Mus

Samples	Wavenumber (cm^{-1})	Vibration mode	Functional group
Mus	3630	Stretching vibration	-OH
	3436	Stretching vibration	-OH
	1645	Stretching vibration	C-C
	1430	Stretching vibration	C-C
	1022	Stretching vibration	Si-O-Si
O-Mus	2940	Antisymmetric stretching vibrations	-OH
	2822	Symmetrical stretching vibrations	-OH
	1480	Stretching vibration	$-C_6H_5$
	783	Stretching vibration	C-H

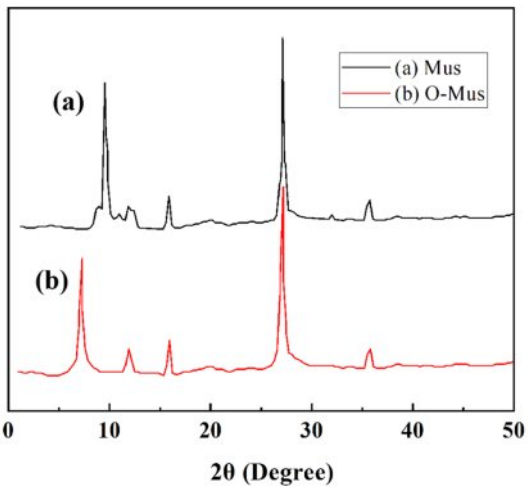

Figure 2. XRD patterns of (a) Mus; (b) O-Mus.

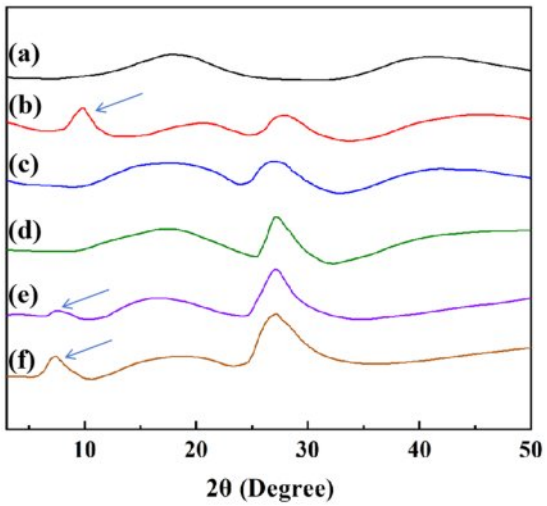

Figure 3. XRD patterns of (a) PCTG; (b) PCTG/Mus-4; (c) PCTG/O-Mus-2; (d) PCTG/O-Mus-4; (e) PCTG/O-Mus-6; (f) PCTG/O-Mus-8.

lamellar structure in PCTG. The characteristic peak of O-Mus did not appear in PCTG/O-Mus-2 (c) and PCTG/O-Mus-4 (d), means O-Mus was stripped and evenly dispersed in PCTG at the addition of 2% and 4%. The characteristic peak of O-Mus appears in PCTG/O-Mus-6 (e), but the intensity is much lower than that of PCTG/O-Mus-8, indicating that when 6% of O-Mus is added to PCTG, O-Mus mainly exists in the stripped state, and only a small amount retained a lamellar structure. When the addition of O-Mus is 8% (f), O-Mus mainly retained lamellar structure in PCTG, which is mainly because the addition of O-Mus is too large and its dispersion in PCTG is not uniform, so cannot achieve the effect of stripping. The structural state of O-Mus within PCTG is shown in Figure 4.

SEM Analysis. It can be seen from Figure 5 that the impact fracture surface of PCTG/Mus-4 (b) had some exposed Mus, and many of them are separated from the PCTG, indicating that the interface link between Mus and PCTG is not strong, and the interface is destroyed when stressed. In contrast to the impact fracture surface of PCTG/Mus-4, the impact fracture surface of PCTG/O-Mus-4 (c) became rougher. Although O-Mus particles were still observable, they were encapsulated by the PCTG matrix. This implies strong interfacial bonding between O-Mus and PCTG. Under external force, the O-Mus did not detach from the matrix, enabling effective stress transfer. Consequently, the fracture surface exhibited characteristics of ductile tearing. In addition, a large number of O-Mus agglomerations were observed on the impact fracture surface of PCTG/ O-MUS-8(d), and they were partially separated from the matrix, indicating that O-Mus agglomerates due to uneven dispersion, resulting in a decrease in the interfacial link strength between O-Mus and PCTG. The analysis of XRD and SEM provided important support for the following analysis of performance.

Dimensional Stability of PCTG Composites. Dimensional stability is an important property index of thermoplastic polymers, which is expressed by moulding shrinkage, post-moulding shrinkage and total shrinkage, especially post-moulding shrink-

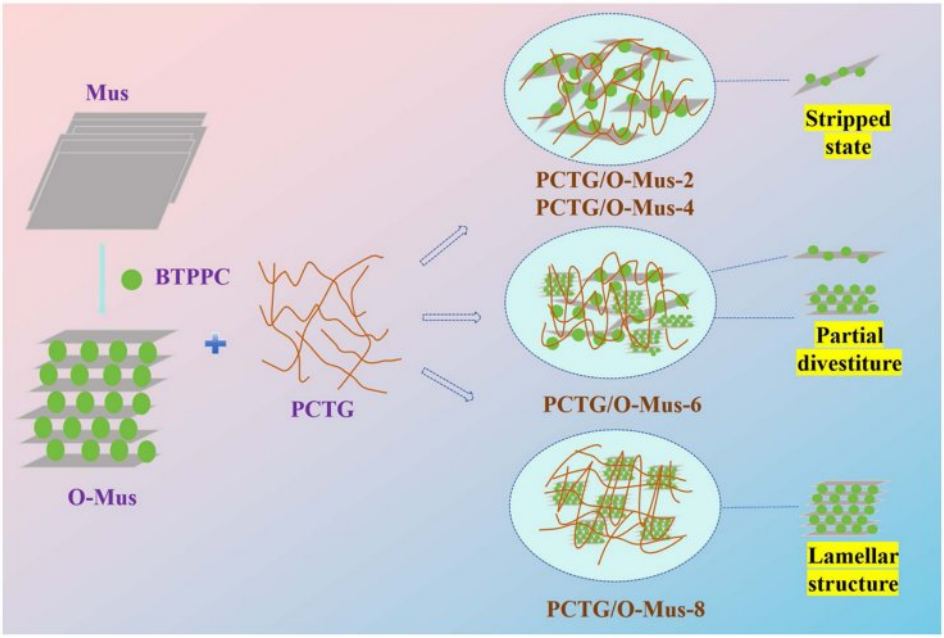

Figure 4. Schematic of the structural state of O-Mus within PCTG.

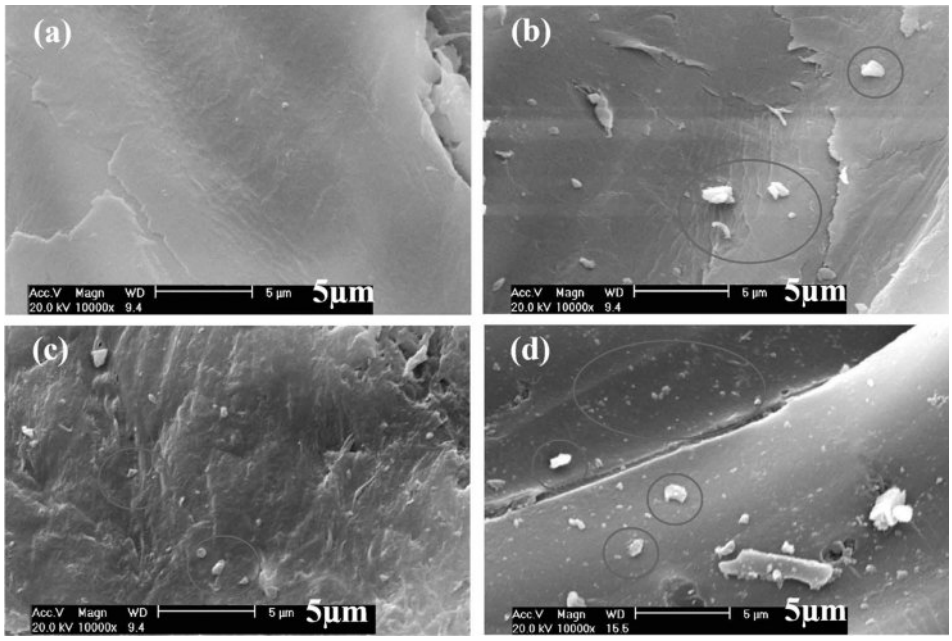

Figure 5. SEM of the impact fracture surface of (a) PCTG; (b) PCTG/Mus-4; (c) PCTG/O-Mus-4; (d) PCTG/O-Mus-8.

age. During the period after injection molding of polymer, the dimensional stability of the product is poor due to the movement of molecules in polymer.[31] Therefore, we can improve the dimensional stability of the product by restraining the movement of molecules of the polymer. Figure 6 showed the percentages of the post-moulding shrinkage (normal and parallel) of PCTG composites. It could be observed that addition of Mus in PCTG let the post-moulding shrinkage parallel to the melt flow direction (PMD) and the post-moulding shrinkage normal to the melt flow direction (NMD) of composites are decreased, and the dimensional stability of PCTG/O-Mus-4 was better than PCTG/Mus-4 because O-Mus has better interfacial compatibility with PCTG compared to Mus. Moreover, the dimensional stability of PCTG/O-Mus increased with increasing O-Mus

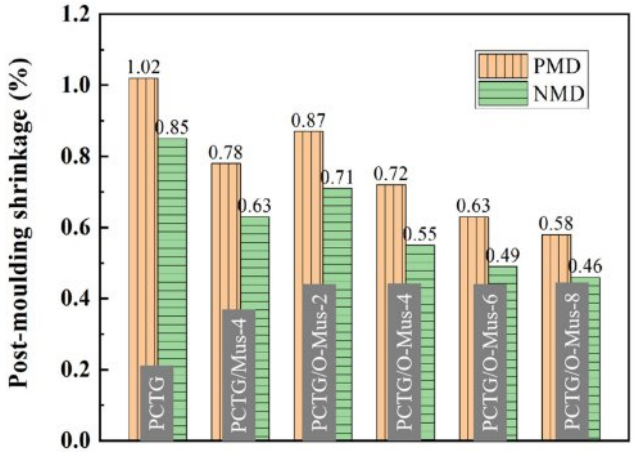

Figure 6. The post-moulding shrinkage of PCTG composites.

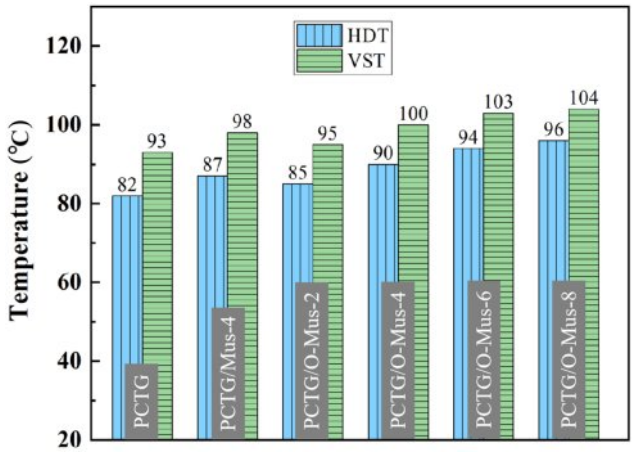

Figure 7. The HDT and VST of PCTG composites.

content in the composites, which might be because that O-Mus restricted motion of polymer chains. The post-moulding shrinkage of PMD and NMD of PCTG/O-Mus-8 were 0.58% and 0.46% respectively, which were 46.12% and 45.9% lower than those of PCTG (1.02% and 0.85%).

HDT and VST of PCTG Composites. When measuring hot deformation temperature (HDT) and vicat softening temperature (VST), the standard test specimen is subjected to a constant load, the temperature is raised at a uniform rate, and the temperature at which the standard deflection, corresponding to the specified in flexural strain or insert the metrics, occurs is measured.[31] Figure 7 showed the deformation temperature and vicat softening temperatur of PCTG composites. Like the dimensional stability of PCTG, the addition of O-Mus into PCTG improved the HDT and VST of composites, the HDT and VST of PCTG/O-Mus-4 was better than PCTG/Mus-4, which might be attributed that O-Mus have better interfacial compatibility with PCTG compared to Mus. Besides, it was observed that the HDT and VST of PCTG/O-Mus also increased with increasing O-Mus content in the composites, the result was attributed that O-Mus can restrict motion of polymer chains, which let the deformation speed of standard spline becomes slower and the composites became stiffer, therefore, the hot deformation temperature and vicat softening temperatur increases under the action of constant pressure. The HDT and VST of PCTG/O-Mus-8 were 96 °C and 104 °C respectively, which were 14 °C and 11 °C greater than those of PCTG (82°C and 93 °C).

DMA of PCTG Composites. DMA analysis was used to assess the effect of the content of O-Mus and the extent of their stripping in PCTG on the thermomechanical properties of the PCTG/O-Mus composites. Figure 8 shows that all PCTG composites show a significant increase in energy storage modulus in the vitrified state relative to pure PCTG. For the composite containing O-Mus, the energy storage modulus of PCTG/O-Mus increases with the increase of O-Mus content, because the interaction between PCTG and O-Mus at the interface hinders the movement of those PCTG molecular chains near the interface. When the composite is subjected to external load, the good interface bonding enables the load to be effectively transferred from the PCTG matrix to the rigid Mus, resulting in the increasing modulus of the PCTG composite in the glassy state.

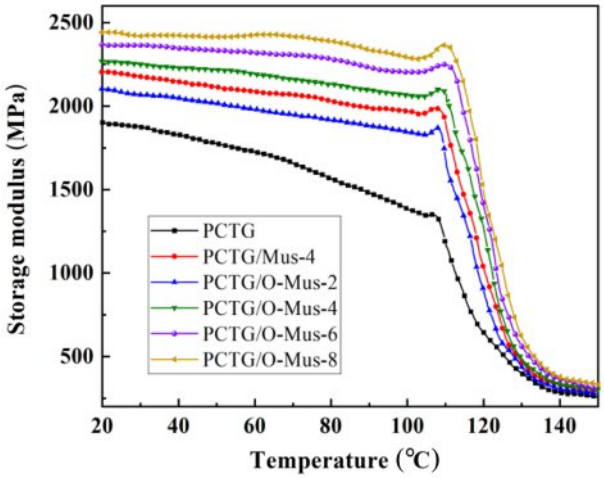

Figure 8. Relationship between storage modulus and temperature of PCTG composites.

The variation of tanδ with temperature reflects the dynamic relaxation behavior of polymer chains and the interfacial interaction between fillers and the matrix. A higher tanδ peak generally corresponds to greater energy dissipation. As shown in Figure 9, the tanδ peak intensity follows the order: PCTG/O-Mus-4 > PCTG/Mus-4. Moreover, the tanδ peak of PCTG/

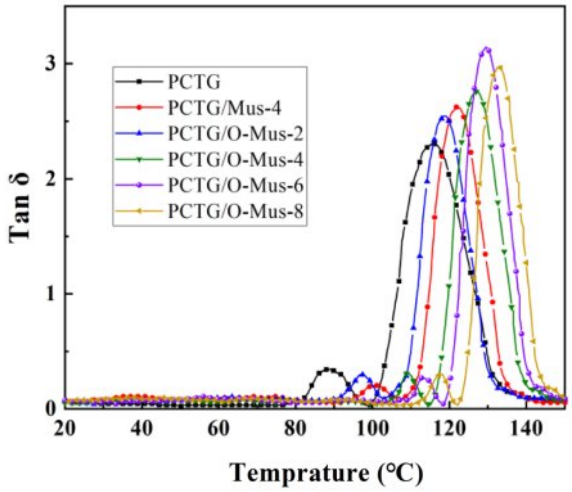

Figure 9. Relationship between tanδ and temperature of PCTG composites.

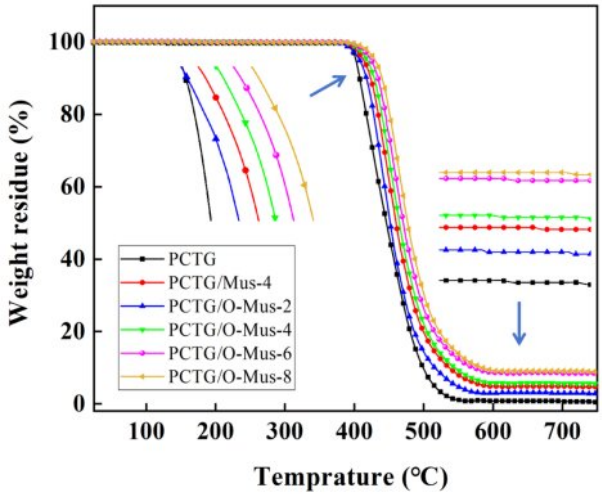

Figure 10. TG curves of PCTG composites.

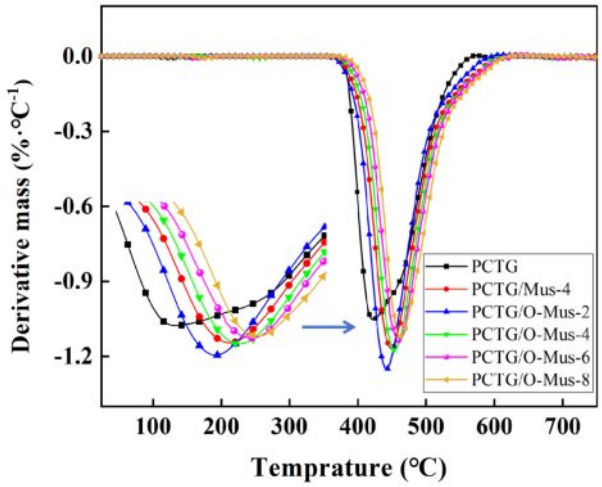

Figure 11. DTG curves of PCTG composites.

O-Mus composites first increases and then decreases with increasing O-Mus loading. This may be attributed to the fact that at low O-Mus loadings, O-Mus is well dispersed in the PCTG matrix, forming a large number of interfacial regions. Under dynamic loading, friction and slippage between the well-dispersed O-Mus and PCTG chains lead to increased energy dissipation, resulting in a higher tanδ peak compared to neat PCTG and PCTG/Mus-4 composites. At high O-Mus loadings, O-Mus agglomerates in the PCTG matrix, reducing the effective interfacial area between the filler and the matrix. The energy dissipation from interfacial slippage is thus significantly suppressed, leading to a decrease in the tanδ peak. In addition, the temperature corresponding to the tanδ peak of PCTG/O-Mus composites gradually increases with the addition of O-Mus, indicating that the glass transition temperature (T_g) of PCTG can be improved by adding O-Mus to PCTG, which is consistent with the test results of HDT.

Thermogravimetry Analysis of PCTG Composites. As observed from Figures 10, Figure 11, and Table 3, the incorporation of O-Mus into PCTG led to a gradual increase in the initial decomposition temperature ($T_{5\%}$) and the temperature at the maximum mass loss rate (T_{max}), and char residue content at 750 °C of the PCTG/O-Mus composites with increasing O-Mus loading. This indicates that O-Mus enhanced the thermal stability of PCTG. This phenomenon may be attributed to O-Mus being a layered, high-temperature-resistant material. Its dispersion within the PCTG matrix can hinder oxygen and heat transfer, thereby increasing the decomposition temperature and high-temperature char residue content[32] of PCTG. PCTG/O-Mus-4 exhibited higher $T_{5\%}$, T_{max}, and char residue content than PCTG/Mus-4. This is attributed to the exfoliated state of O-Mus within the PCTG matrix, which resulted in superior dispersion and enhanced interfacial compatibility with PCTG compared to Mus. With an 8% O-Mus loading, PCTG/O-Mus-8 exhibited $T_{5\%}$ and T_{max} of 429.2 °C and 433.3 °C, respectively. These represent increases

Table 3. TG Characteristic Data of PCTG Composites

Sample	$T_{5\%}$ (°C)	T_{max} (°C)	Char residue at 750 °C (%)
PCTG	401.2	422.3	0.49
PCTG/Mus-4	413.4	449.1	4.72
PCTG/O-Mus-2	407.5	441.9	2.83
PCTG/O-Mus-4	418.7	453.5	5.49
PCTG/O-Mus-6	423.8	460.1	8.46
PCTG/O-Mus-8	429.2	463.3	8.93

of 28.0 °C and 41.0 °C compared to neat PCTG.

Mechanical Properties of PCTG Composites. The mechanical properties of PCTG composites were shown in Table 4. It could be observed that the flexural strengths and tensile strengths of PCTG/Mus-4 increased compared with PCTG, and it came to 78.4 MPa and 62.2 MPa, which was 8.4% and 10.3% more than that of PCTG (72.3 MPa and 56.4 MPa). The enhanced performance is mainly attributed to the homogeneous dispersion of Mus in the PCTG matrix and their favorable interfacial adhesion, which facilitates efficient stress transfer between PCTG and Mus. It was also observed that the flexural modules of PCTG/Mus-4 came to 2314.8 MPa, which was 12.9% more than PCTG (2050.6 MPa), nevertheless, the elongation at break and notched izod impact strength of PCTG were reduced when added Mus.

This phenomenon is primarily attributed to the layered silicate structure of Mus, wherein PCTG molecular chains intercalate into the interlayer spaces of Mus. This intercalation enhances the interfacial bonding strength between PCTG and Mus, consequently restricting the mobility of PCTG molecular chains and leading to reduced ductility of the composite material. The mechanical properties of PCTG/O-Mus-4 were better than PCTG/Mus-4, because O-Mus was modified by BTPPC, which led O-Mus to have better interfacial adhesion with PCTG than Mus, and better adhesion resulted in turn increased stress transfer from matrix to O-Mus and increasing mechanical properties. This is consistent with the SEM analysis of the impact fracture surface.

The deformation capacity of the polymer was decreased and the materials became stiffer when the polymer chains were restricted to move, resulting in an increase in the flexural modulus modulus of composites increased. Figure 12 showed the effect of O-Mus content on the flexural properties of PCTG/O-Mus composites. The flexural modulus of PCTG/O-Mus increased with increasing content of O-Mus, indicating that the O-Mus restricting polymer chains to move, the materials became stiffer. The flexural strengths of PCTG/O-Mus increased with adding O-Mus when the content of O-Mus was less than 6%, which was attributed that the low content of O-Mus had homogeneous dispersion and exists mainly in the peeled state in the PCTG, and has a strong interface link with the PCTG. However, the flexural strengths of PCTG/O-Mus decreased when the content of O-Mus was more than 6%, because O-Mus was agglomerated and exists mainly in a layered structure in PCTG. This is consistent with the analysis of SEM and XRD.

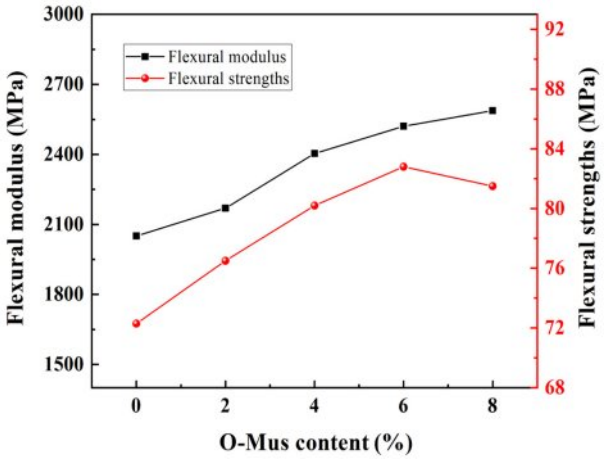

Figure 12. Effect of O-Mus content on the flexural properties of PCTG composites.

The addition of O-Mus into PCTG deleteriously affected the notched izod impact strength and elongation at break of the composites. As shown in Figure 13, both properties decrease monotonically with increasing O-Mus content, with a particularly sharp drop at high loadings. This phenomenon can be attributed to: First, the rigid O-Mus nanosheets dispersed in the PCTG matrix strongly restrict the segmental motion and long-range relaxation of polymer chains, reducing the plastic deformation capacity of the matrix and the ductility of the composites. Second, with the increase of O-Mus content, filler agglomeration becomes more severe, and the aggregated particles act as significant stress concentration points, which promote the initiation and rapid propagation of cracks under external force, leading to a transition from ductile to brittle fracture. Third, the accumulation of interfacial microvoids and defects at high filler loadings further weakens the interfacial bonding strength, accelerating

Table 4. Mechanical Properties of PCTG Composites

Samples	Mechanical properties				
	Flexural modules (MPa)	Flexural strengths (MPa)	Tensile strengths (MPa)	Elongation at break (%)	Notched Izod impact strength (kJ/m^2)
PCTG	2050.6±8	72.3±3	56.4±3	250.3±5	80.2±4
PCTG/Mus-4	2314.8±10	78.4±3	62.2±2	190.4±7	67.2±2
PCTG/O-Mus-4	2403.7±10	80.2±2	63.8±2	220.5±5	74.5±2

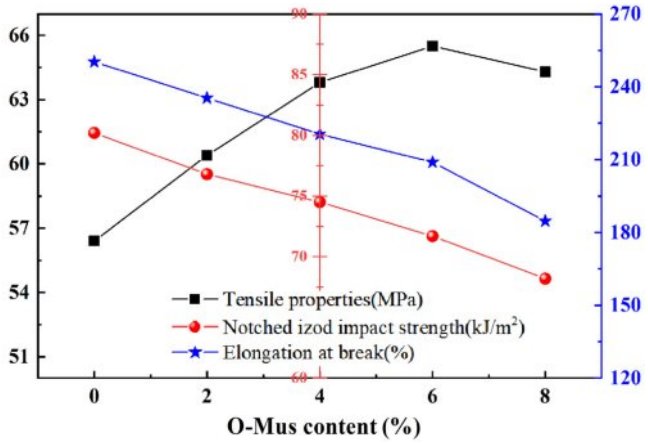

Figure 13. Effect of O-Mus content on the tensile properties and notched izod impact strength of PCTG composites.

material failure. Similar to the flexural strength, the tensile strength of PCTG/O-Mus composites initially increases and then decreases. This phenomenon can be mainly explained as follows: At low O-Mus loadings, the filler is mainly exfoliated in the PCTG matrix, with a large specific surface area and good interfacial bonding with PCTG, resulting in efficient stress transfer between O-Mus and PCTG, thus increasing the tensile strength. In contrast, at high O-Mus loadings, agglomeration occurs in the PCTG matrix, which weakens stress transfer and leads to a decrease in tensile strength.

Light Transmittance and Chemical Resistance of PCTG Composites. It can be seen from Table 5 that with the addition of O-Mus to PCTG, the light transmittance of the composite material gradually decreases as the O-Mus loading increases. This is because O-Mus is a non-transparent inorganic layered structure dispersed in PCTG, which hinders the transmission of light. In addition, it can be seen from the table that the addition of O-Mus has no effect on the alkali resistance of PCTG.

Conclusions

In conclusion, Mus was organically modified with BTPPC first, and then obtained O-Mus was used to prepare a series of PCTG/O-Mus composites. FTIR and XRD analysis showed that Mus was successfully organically modified and BTPPC was intercalated between Mus layers. When the addition amount of O-Mus was 2%, 4% and 6%, the O-Mus was mainly in a delaminated state and well dispersed in PCTG. SEM analysis indicated that the interfacial bonding strength was in the order of PCTG/O-Mus-4 > PCTG/Mus-4. The dimensional stability, hot deformation temperature (HDT), vicat softening temperature (VST) and thermal decomposition temperature of PCTG/O-Mus increased with increasing the content of O-Mus. The flexural modulus of PCTG/O-Mus was improved and the notched izod impact strength and elongation at break were reduced when O-Mus was added into PCTG. The flexural and tensile strengths of PCTG/O-Mus increased at first (O-Mus content was under 6%), and then decreased (O-Mus content was up 6%), indicating O-Mus at higher content began to gather and had poor dispersion in PCTG. The PCTG/O-Mus-6 composites have better dimensional stability, hot deformation temperature (HDT), vicat softening temperature (VST), decomposition temperature and comprehensive mechanical properties when the addition amount of O-Mus was 6%.

Table 5. Light Transmittance and Chemical Resistance of PCTG Composites

Sample	Light transmittance/%	Chemical resistance (PH 11, 5d)
PCTG	90.2	no visible change
PCTG/Mus-4	80.5	no visible change
PCTG/O-Mus-2	88.7	no visible change
PCTG/O-Mus-4	85.2	no visible change
PCTG/O-Mus-6	77.3	no visible change
PCTG/O-Mus-8	65.6	no visible change

Acknowledgment: We would like to thank a Project Supported by Scientific Research Fund of Hunan Provincial Education Depart ment (NO. 25B1032) and Aid Program for Research and Innova tion Team in Hunan Chemical Vocational Technology College (NO. HNHYTD202510).

Conflict of Interest: The authors declare that there is no conflict of interest.

References

1. Song, H. J.; Chen, X. D.; Fan, J. C. Balanced Strength and Toughness Improvement in Polylactide (PLA)/poly(1,4-cyclohexylene dimethylene terephthalate glycol) (PCTG) Blends Using Various Compatibilizers. *Iran. Polym. J.* **2019**, 28, 991-999.
2. Granado, A.; Iturriza, L.; Eguiazábal, J. I. Structure and Mechanical Properties of Blends of an Amorphous Polyamide and an Amorphous Copolyester. *J. Appl. Polym. Sci.* **2014**, 131, e40785.
3. Auerbach, A. B.; Sell, J. W. Evaluation of Poly(1,4cyclohexylene dimethylene terephthalate) Blends for Improved Processabilit.

Polym. Eng. Sci. **1900**, 38, 1041-1050.
4. Lee, P. C.; Ha, J. U.; Kim, S. Y. Effects of Temperature and Nano-filler Content on Water Uptake in Nanocomposites. *Polym. Korea* **2019**, 43, 584-588.
5. Borralleras, P.; Segura, I.; Aranda, M. A. G. Influence of the Polymer Structure of Polycarboxylate-based Superplasticizers on the Intercalation Behaviour in Montmorillonite Clays. *Constr. Build. Mater.* **2019**, 220, 285-296.
6. Krikorian, V.; Pochan, D. Poly(l-lactide acid)/layered Silicate Nanocomposite: Fabrication, Characterization, and Properties. *Chem. Mater.* **2003**, 15, 4317-4324.
7. Furuhashi, Y.; Morioka, K.; Tamegai, H.; Yoshie, N. Preparation and Some Properties of Stereocomplex-type Poly(lactic acid)/layered Silicate Nanocomposites. *J. Appl. Polym. Sci.* **2013**, 127, 1615-1622.
8. Moll, J. F.; Akcora, P.; Rungta, A. Mechanical Reinforcement in Polymer Melts Filled with Polymer Grafted Nanoparticles. *Macromolecules* **2011**, 44, 7473-7477.
9. Seo, S. D.; Kang, K. C.; Jeong, J. W. Preparation and Characterization of Poly Methyl Methacrylate/Clay Nanocomposite Powders by Microwave-Assisted In-Situ Suspension Polymerization. *J. Nanosci. Nanotechno* **2020**, 20, 4193-4197.
10. Scalfaro, R.; Mistretta, M. C.; Lamantia, F. P. Compatibilized Polyamide 6/Polyethylene Blend-Clay Nanocomposites: Effect on the Degradation and Stabilization of the Clay Modifier. *Polym. Degrad. Stab*. **2008**, 93, 1267-1274.
11. Karimzadeh, I.; Sabzi, M.; Safibonab, B. Improving Environmental Durability of Epoxy Resin Using Tetra-n-butylammonium (TBA) Salt Modified Montmorillonite Nanoplatelets. *Polym. Korea* **2017**, 41, 98-103.
12. Cui, L.; Khramo, D. M.; Bielawski, C. W. Effect of Organoclay Purity and Degradation on Nanocomposite Performance, Part 1: Surfactant Degradation. *Polymer* **2008**, 49, 3751-3761.
13. Shelley, J. S.; Mather, P. T.; DeVries, K. L. Reinforcement and Environmental Degradation of Nylon 6/clay Nanocomposites. *Polymer* **2002**, 42, 5849-5858.
14. Lee, E. J.; Yoon, Y. K.; Lim, K. H. Silanized Montmorillonite Capsule and Functional Materials Filled Hybrid Polymer-modified Waterproofing Asphalt. *Polym. Korea* **2020**, 44, 672-683.
15. Granado, A.; Eguiazabal, J. I.; Nazabal, J. J. Effects of the Processing Temperature on the Nanostructure and Mechanical Properties of PCTG-Based Nanocomposites. *Appl. Polym. Sci*. **2011**, 127, 136-144.
16. Huang, J. C.; Zhu, Z. K.; Yin, J. Poly(etherimide)/montmorillonite Nanocomposites Prepared by Melt Intercalation: Morphology, Solvent Resistance Properties and Thermal Properties. *Polymer* **2011**, 42, 873-877.
17. AAzeez, A. A.; Rhee, K. Y.; Park, S. J. Epoxy Clay Nanocomposites - Processing, Properties and Applications: A Review. *Compos. Part B-Eng.* **2013**, 45, 308-320.
18. Kornmann, X.; Lindberg, H.; Berglund, L. A. Synthesis of Epoxy–clay Nanocomposites: Influence of the Nature of the Clay on Structure. *Polymer* **2001**, 42, 1303-1310.
19. Azad, A. K.; Unnikrishn, L.; Mohanty, S. Nanomaterial Enhanced Polyelectrolyte Membranes for Hydrogen-Oxygen Fuel Cells. *Polym. Korea* **2021**, 45, 101-112.
20. Gudivada, G.; Kandasubramanian, B. Polymer-phyllosilicate Nanocomposites for High-temperature Structural Application. *Polym-Plast. Technol.* **2020**, 59, 537-591.
21. Wang, K. H.; Choi, M. H.; Koo, C. M. Synthesis and Characterization of Maleated Polyethylene/clay Nanocomposites. *Polymer* **2001**, 42, 9819-9826.
22. Ray, S. S.; Bousima, M. Biodegradable Polymers and Their Layered Silicate Nanocomposites: in Greening the 21st Century Materials World. *Prog. Mater. Sci*. **2005**, 50, 962-1079.
23. Li, Y.; Sun, H. J.; Peng, T. J. Effects of Muscovite Matrix on Photocatalytic Degradation in TiO_2/muscovite Nanocomposites. *Appl. Clay. Sci* **2019**, 179, e105155.
24. Li, Y.; Sun, H. J.; Peng, T. J.; You, H.; Zeng, L.; Qin, Y. T. Preparation and Visible Photocatalytic Properties of N-doped TiO_2/muscovite Nanocomposites. *Clay. Clay. Miner.* **2021**, 69, 254-262.
25. Sathyamoorthy, G.; Raghunathan, V.; Rangappa, S. M. Exploring the Tribological Impact of Micaceous Additives in Copper-free Automobile Brake Friction Composites. *J. Vinyl. Addit. Technol.* **2025**, 31, 279-297.
26. Chen, Y. C.; Cheng, Y. C.; Ke, W. E. Creation of Novel Composite: Flexible Magnetic and Conductive Muscovite. *Mater. Today. Adv.* **2023**, 20, e100423.
27. Zhang, L.; Wei, T.; Chen, H.; Lai, W. Mechanical and Thermal Properties of Muscovite and Density Polyethylene-reinforced and -toughened Polypropylene Composites. *J. Wuhan. Univ. Technol.* **2009**, 24, 581-587.
28. Ismail, N. H. C.; Akil, H. M. ABS/Nonexpandable Muscovite Clay Nanocomposites: The Effect of Ion Exchange on Dispersion of Nanofillers and Flexural Properties. *Polym. Composite* **2019**, 40, 3562-3572.
29. Simons, R.; Qiao, G. G.; Bateman, S. A. Direct Observation of the Intergallery Expansion of Polystyrene-Montmorillonite Nanocomposites. *Chem. Mater.* **2011**, 23, 2303-2310.
30. Nikolaidis, A. K.; Achilias, D. S.; Karayannidis, G. P. Synthesis and Characterization of PMMA/Organomodified Montmorillonite Nanocomposites Prepared by in Situ Bulk Polymerization. *Ind. Eng. Chem. Res* **2011**, 50, 571-579.
31. Li, X.; Fang, S. G.; Yin, J.; Xu, J. Utilization the Synergistic Effect of Talcum Powder and Bamboo Charcoal to Modify PP with Higher Dimensional Stability and Hot Deformation Temperature. *Polym. Korea* **2021**, 45, 340-345.
32. Li, X.; Wang, G. R.; Wang, Z. L. Fabrication of Thin-walled Flame-retardant Recycled Polyethylene Composites: Synergistic Flame Retardancy of Muscovite in APP/MCA Systems. *Polym. Degrad. Stabil.* **2025**, 241, 111561.

Publisher's Note The Polymer Society of Korea remains neutral with regard to jurisdictional claims in published articles and institutional affiliations.